

# Modeling Approaches for Controller Design using the Example of a Valve-driven Force-controlled Bearing Preload Element

Georg Ivanov, Christian Rutter, Thomas Reuter and Thomas Burkhardt

ICM – Institut Chemnitzer Maschinen- und Anlagenbau e.V., Otto-Schmerbach-Str. 19, Chemnitz, Germany

**Keywords:** System Simulation, Modeling Approaches, Controller Development, Bearing Preload, CNC-Spindle.

**Abstract:** Conventional machine tool spindles are factory-equipped with a fixed bearing preload. Depending on the preload level, the field of application of a machine tool is limited to certain processing tasks. As part of a collaborative project between ICM e.V., Spindel- und Lagerungstechnik Fraureuth GmbH and SITEC Automation GmbH, funded by the European funding initiative EFRE, a novel adaptronic machine tool spindle has been developed. The new spindle offers the possibility of a variable adjustment of the bearing preload, whereby the machining spectrum of the machine tool can be significantly expanded. The functional principle is a rotationally symmetrical hydraulic bearing preload element integrated in the main spindle. By changing the pressure in the oil filled preload element, a relative displacement of the bearing rings is caused. The bearing preload can be varied proportionally to the relative bearing stroke. Aim of the investigation was to compare different levels of detail in modeling the main system components and the overall control system for the purpose of controller development. Therefore the Modelica-based simulation environment SimulationX® was used.

## 1 INTRODUCTION

Figure 1 shows an adaptronic main spindle for CNC lathes developed at ICM e.V. The stepless adjustment of the bearing preload takes place according to (Ivanov, 2018) via a rotationally symmetrical preload element integrated between housing and spindle shaft.

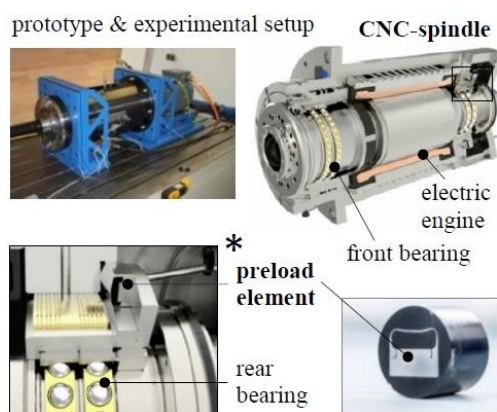


Figure 1: Structure and functional principle of the adaptronic main spindle developed at ICM e.V., based on (Ivanov, 2018).

By varying the oil pressure, a deformation of the preload element membrane is caused. The stroke of the preload element thus produced is transmitted on the outer ring of the rear roller bearing via a Z-bushing. The relative displacement between inner and outer ring causes an axial bracing on the bearings. The preload force can therefore be controlled via the stroke of the preload element.

Core of the current investigation was the comparison of different modeling approaches for mapping control loop components and the overall control loop in a system simulation environment. The aim was to investigate how different modeling approaches of the main components and the overall control system affect the model accuracy, in particular the closed-loop behavior, and the simulation performance.

## 2 MODELING APPROACHES FOR 4/3-WAY CONTROL VALVES

Three control valve models have been compared with measured data according to their model accuracy. The investigation included an analytical

model based on the flow-load-function according to (Weber, 2011), a model based on the measured 3D-flow-maps of the different control edges and an analytical model from the model library of the used simulation program (SimulationX®).

## 2.1 Flow-load Model

The transmission behavior of the control valve can be subdivided into its dynamic (valve spool movement) and its static (flow behavior) transmission behavior. The temporal course of the spool position can be described according to (Weber, 2011) by a second order differential equation (PT2 element):

$$\frac{1}{\omega_{0V}^2} \cdot \ddot{y} + \frac{2D}{\omega_{0V}} \cdot \dot{y} + y = K_{yV} \cdot U \quad (1)$$

$\omega_{0V}$  is the characteristic frequency of the undamped oscillation of the control valve,  $D$  the damping ratio and  $K_{yV}$  the valve gain. The solution of the differential equation gives the temporal course of the spool position as a function of the control valve voltage. The flow behavior of the control valve can be described in simplified terms with the flow-load function according to (Weber, 2011). For an application-specific description of the flow behavior when the consumer port B is blocked, the description of the two control edges P-A and A-T is sufficient:

$$Q_{P-A} = Q_{nom} \cdot \frac{y_{0P-A} + y}{y_{max}} \cdot \sqrt{\frac{p_P - p_A}{p_{nom}}} \quad (2)$$

$$Q_{A-T} = Q_{nom} \cdot \frac{y_{0A-T} - y}{y_{max}} \cdot \sqrt{\frac{p_A - p_T}{p_{nom}}} \quad (3)$$

Therefore  $p_P$  designates the system pressure before the control valve,  $p_A$  the pressure at the consumer connection A,  $y$  the current spool position and  $y_{max}$  the maximum spool position. The two constants  $y_{0P-A}$  and  $y_{0A-T}$  take into account the different overlap ratios of the control edges. The nominal volume flow  $Q_{nom}$  and the nominal pressure  $p_{nom}$  have been determined metrologically. The volume flow at the consumer connection of the control valve results from the difference between the two control edge flows:

$$Q_A = Q_{P-A} - Q_{A-T} \quad (4)$$

## 2.2 Measurement based 3D-Map-model

The mapping of the dynamic transfer behavior is equivalent to the analytical model. The static transmission behavior is realized by implementing the experimentally determined 3D-flow-maps of the two control edges P-A and A-T in the model. The 3D-flow-maps match the following form:

$$Q_{P-A} = f(y, dp_{P-A}) \quad (5)$$

$$Q_{A-T} = f(y, dp_{A-T}) \quad (6)$$

The volume flow at the consumer connection is calculated according to equation (4). For a realistic application-specific mapping of the control valve, its flow behavior in the small signal range (between -1 to 1 V) is particularly important. Background is the high pressure gain of the control valve.

## 2.3 SimulationX-model

The mapping of the dynamic transmission behavior is analogous to the analytical model described above. The control valve model of the used simulation software (SimulationX®) is based on the orifice formula - see for example (Hatami, 2013).

$$Q = \alpha \cdot \sqrt{\frac{1}{\rho_{oil}}} \cdot A \cdot \sqrt{p_{in} - p_{out}} \quad (7)$$

For each control edge of the control valve, the flow is calculated separately. The maximum flow cross sections of the control edges are calculated on the basis of simplifying assumptions from the metrologically determined nominal flow rate, the nominal pressure and the oil density during the experimental investigation of the valve.

$$A = \frac{Q_{nom}}{\alpha_T} \cdot \sqrt{\frac{\rho_{ref}}{2 \cdot p_{nom}}} \quad (8)$$

For calculating the flow coefficient  $\alpha$ , a case differentiation between laminar and turbulent flow takes place:

$$\alpha = \begin{cases} \frac{1}{\sqrt{\zeta}} & \text{for } Re \leq Re_K \\ \alpha_T & \text{for } Re \gg Re_K \end{cases} \quad (9)$$

Here  $Re_K$  marks the critical Reynolds number and  $\alpha_T$  a constant value for the flow coefficient in the turbulent range. The Reynolds number  $Re$  is calculated from the current volume flow  $Q$  over the respective control edge, the hydraulic diameter  $d_h$ ,

the flow cross section  $A$  of the control edge and the kinematic oil viscosity  $\nu$ .

$$Re = \frac{Q \cdot d_h}{A \cdot \nu} \quad (10)$$

For calculating the hydraulic diameter, a circular geometry of the flow cross section of the control edges is assumed.

$$d_h = \sqrt{\frac{4 \cdot A}{\pi}} \quad (11)$$

The calculation of the pressure loss factor  $\zeta$  is based on the equation for sharp-edged circular orifices given by (Töpfer and Schwarz, 1988):

$$\zeta = \left( \frac{1}{\mu} - \frac{A_2}{A_1} \right)^2 \quad (12)$$

The determination of the contraction coefficient  $\mu$  also takes place according to (Töpfer and Schwarz, 1988) via an empirical formula:

$$\mu = 0,598 + 0,395 \cdot \left( \frac{A_2}{A_1} \right)^2 \quad (13)$$

## 2.4 Comparison of Modeling Approaches for Control Valves

Figure 2 shows a comparison of the simulation results of the three control valve models with the results of the metrological characterization of the control valve. The highest accuracy can be achieved with the measurement based 3D-map-model. The model inaccuracy is - except very low pressures - less than 5 % in the entire operating range. Therefore the flow pressure drop characteristic (left, control edge P-A) and the pressure gain characteristic (right) of the different valve models have been compared to the measured data.

With the analytical model based on the flow-load function, model accuracies of up to 95% can be achieved. The lowest model accuracy is provided by the SimulationX@-own valve model. The disadvantage of the flow-load-model and the 3D-map-model, however, is that no dependence of the transfer behavior on the oil viscosity and the temperature can be represented. These models are only valid for certain temperature conditions of the hydraulic system, while the SimulationX model takes the viscosity dependence of the flow behavior into account.

Figure 3 shows a comparison of simulated and metrologically recorded frequency responses and step responses of the control valve. The dynamic

valve behavior, especially in the interesting small signal range, can be mapped very well by a PT2 element. Amplitude ratio and phase lag can be reproduced realistically in the complete frequency range for small input signals. For larger input signals, the model lags behind the real valve. This is also confirmed by the comparison of the model step responses with the measured data. For the controller design, the small signal range is of superior importance. For the parameterization of the models the characteristic frequency and the damping ratio of the small value range should be used.

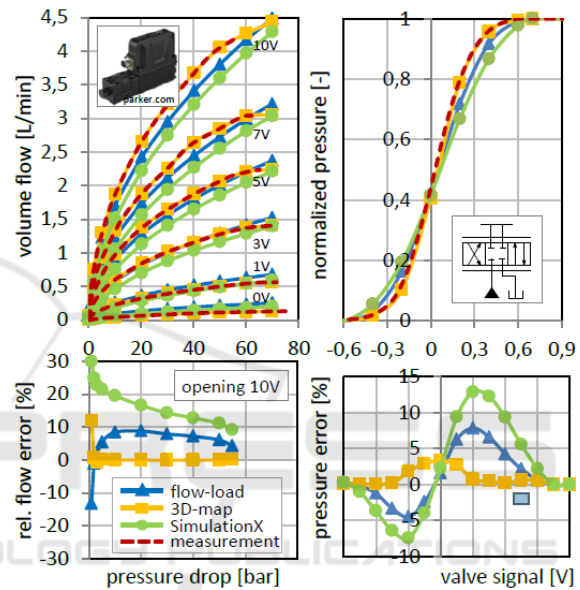


Figure 2: Comparison of the static transmission behavior of different control valve models with measurement results.

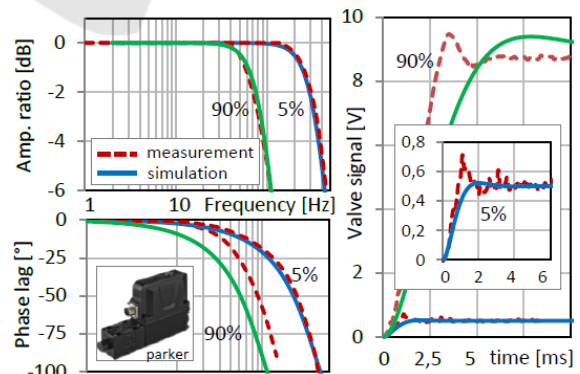


Figure 3: Comparison of the dynamic transmission behavior of control valve models with measurement results, left: frequency responses, right: step responses.

### 3 MODELING OF PRELOAD ELEMENT AND SPINDLE-BEARING SYSTEM

For the overall mapping of the controlled system, the valve driven hydraulic bearing preload element and the spindle bearing system are to be modeled. The preload element can be described according to (Ivanov, 2018) as a coupling of plunger cylinder and spring-damper element. The spring stiffness of the preload element was determined experimentally. The effective piston area of the element was assumed to be constant and generated from the CAD data. The transfer behavior of the preload element can be described, by disregarding the element membrane mass:

$$F_{Pre} = A_{PE} \cdot p_{PE} - c_{PE} \cdot \dot{x} - d_{PE} \cdot \ddot{x} \quad (14)$$

The spring stiffness is in multi-dimensional dependence on the preload element stroke and the acting load force (the acting preload force). The damping was assumed to be constant and has been estimated.

$$c_{PE} = f(x, F_{Pre}) \quad (15)$$

The spring force dependence on stroke and load of the preload element could be determined experimentally and can be described by an approximation function of the following form:

$$F_{PEdis} = a + bx_{PE} + cx_{PE}^2 + dF_{Pre} + eF_{Pre}^2 \quad (16)$$

The spindle-bearing system can be described according to (Ivanov, 2018) by linked spring-damper elements. The axial stiffness-stroke curves of the rolling bearing models used in the prototype were calculated on the basis of a theoretical model according to (Harris, 2001) and then compared with experimental results. To describe the transmission behavior of the spindle-bearing system, the following equation can be used taking into account the spindle inertia.

$$F_{Pre} = c_{sp}(x) \cdot x + b_{sp} \cdot \dot{x} + m_{sp} \cdot \ddot{x} \quad (17)$$

Therefore  $c_{sp}$  is the total stiffness and  $b_{sp}$  is the total damping of the spindle-bearing system. The axial spring force curves of the individual rolling bearings can be described regarding to (Harris, 2001) by third degree polynomials:

$$F_{CB} = c_{B1} \cdot x_{Brel}^3 + c_{B2} \cdot x_{Brel}^2 + c_{B3} \cdot x_{Brel} \quad (18)$$

Figure 4 shows a comparison of measurement and simulation results of the preload element. The experimentally determined stiffness characteristic of the preload element was approximated by a three-

dimensional approximation function (left) and by a simple linear function (right). Figure 4 - below - shows the relative errors between the measured and approximated spring force characteristics of the preload element. With the multi-dimensional approximation function, a very high agreement with the measurement results can be achieved. The maximum relative error in the considered value range is less than 5%. By approximating the spring force characteristic by means of a simple linear function also very high matches can be achieved in a wide value range. With negative strokes (compression of the preload element) and very large strokes the accuracy decreases progressively.

Both approximation functions were used to parameterize the simulation model. Figure 4 - top - shows a comparison of the simulation results of the differently parameterized models with measurement results. In the experiment the pressure in the element was increased while a constant external load force was acting. Thereby the preload element pressure, the stroke and the load force have been measured. It could be shown that – in the interesting value range – the model accuracy cannot be significantly improved by the application of a multi-dimensional approximation function.

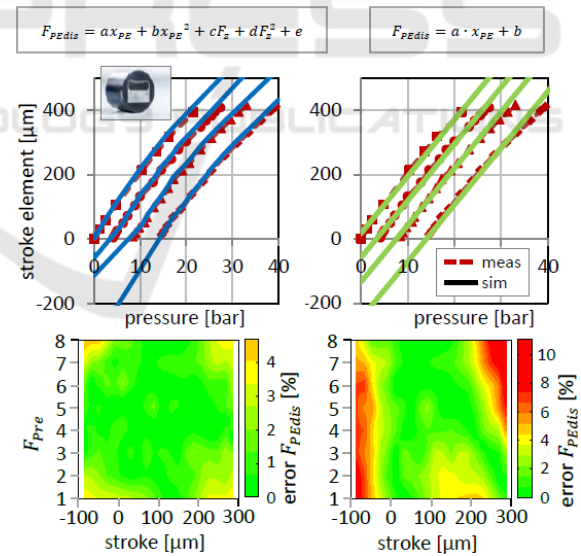


Figure 4: Comparison of measurement and simulation results (top) and the spring force of the preload element (bottom), left: three-dimensional approximation function, right: linear function.

The comparison of measurement and simulation results of the axial spring force curves of the individual spindle bearings shows significant

deviations – see Figure 5, left. These are due to the applied indirect measurement method.

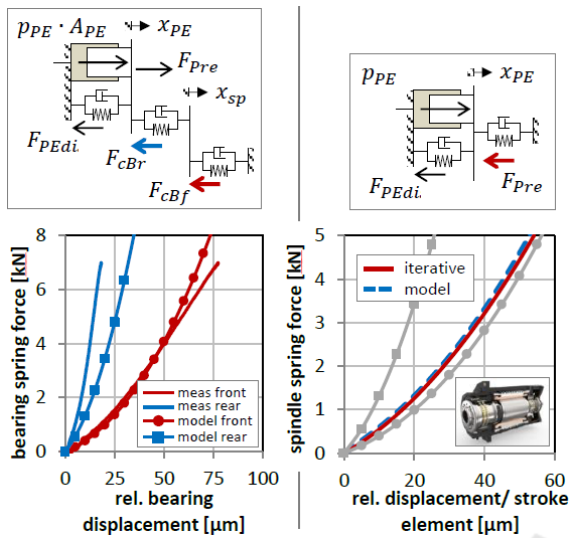


Figure 5: Left - comparison of bearing force curves from measurement and theoretical calculation model (Ivanov, 2018), right - comparison of spindle force curve from iterative calculation and SimulationX model.

Since no force measurement is provided in the prototype spindle, the axial bearing spring forces had to be calculated indirectly from the measured preload element stroke, the measured spindle stroke and the preload element pressure using equation (15). The resulting inaccuracies lead to the strong deviations to the calculated bearing spring force curves. A more accurate measurement of the spindle bearings should be made on the single bearing with direct force measurement. To parameterize the detail model presented in chapter 4, the results of the theoretical calculation model have been used. The axial bearing damping was assumed to be constant according to (Backhaus, 2008).

Figure 5 - right shows the determined total spring force curve of the spindle. The spindle force curve was at first generated on the basis of a simplified iterative calculation and secondly by using the SimulationX model parameterized with the bearing force curves. The material stiffness of the spindle shaft itself was neglected. In the range of interest, only slight deviations between the two approaches can be observed. For the parameter-ization of the signal flow model presented in point 4, the iteratively determined curve was used.

## 4 CONTROL LOOP MODELING APPROACHES

For the design of an optimal force controller, two simulation models of the control loop have been developed on the basis of the previously given analytical descriptions, a detailed physical simulation model a) and a simplified signal flow model b) - see Figure 5. The parameterization of the physical detail model was based on two-dimensional curves, three-dimensional maps and approximation functions which were calculated from the experimentally determined data of the three main components.

Table 1: Parameterization differences between detail model and simplified signal model.

parameter	detail model	signal model
pressure supply	pump with pressure relief valve	constant pressure default
control valve static	3D-maps for control edges P-A and A-T	flow-load-function
force preload element	3D-approx-imation function	linear function
force of spindle bearings	single bearing spring forces	resulting spindle spring force

The parameterization of the signal flow model was based on the analytical flow-load function for the description of the control valve and simplified approximation functions for mapping the preload element and the spindle-bearing system. Important parameterization differences of the two models are summarized in Table 1.

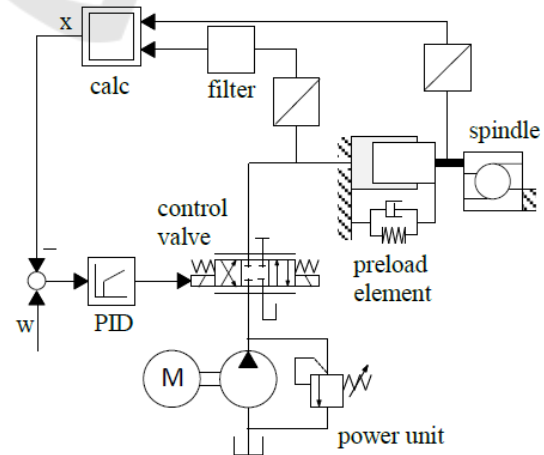


Figure 6: Structure of physical detail model.

Figure 6 shows the basic structure of the physical control system and the developed detailed simulation model and Figure 7 the structure of the simplified signal flow model of the control system.

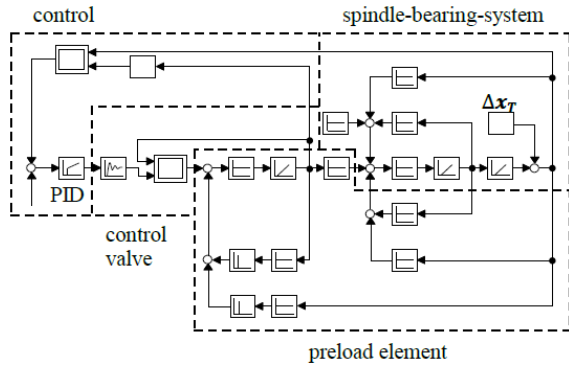


Figure 7: Structure of simplified signal flow model.

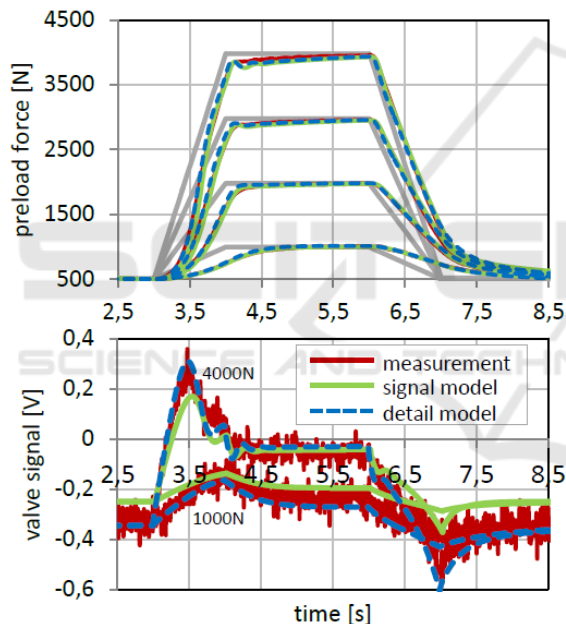


Figure 8: Validation and comparison of simulation accuracy of the detail model and the simplified signal flow model.

Figure 8 shows a comparison of simulation and measurement results for ramp-shaped control inputs. The parameterization of the PID controller took place through systematic trial and error in the experiment.

The control variable and the valve control signal curves show that a high degree of conformity of the detail model with the real system could be achieved. The simulation results of the simplified signal flow model show minor static deviations. To increase the signal model accuracy, the parameterization of the

control valve model had to be adapted. Figure 9 shows the approximation of the pressure-signal curve to the experimentally determined curve by shifting the control edge ratios of the flow-load valve model.

The experimentally determined negative control edge coverage of 0.6 V for P to A and 0.7 V for A to T were set to 0.45 V and 0.5 V. The reparameterization leads to a significantly higher model accuracy with respect to the controlled variable curves, but to slightly higher deviations of the control signal curves of the simplified model.

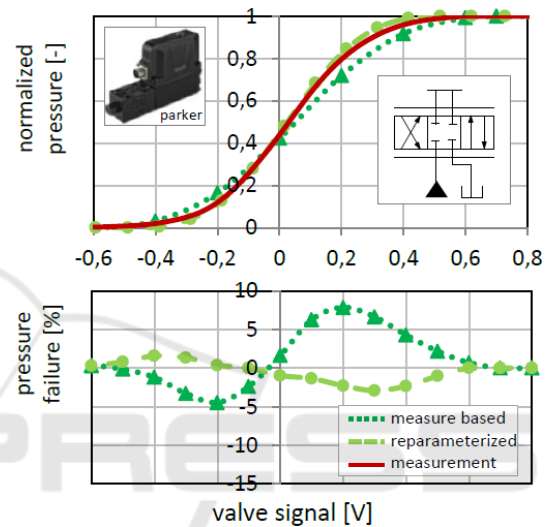


Figure 9: Reparameterization of the flow-load valve model for increasing the signal flow model accuracy.

## 5 PERFORMANCE COMPARISON

Figure 10 shows a comparison of the simulation time of the detailed model and the simplified signal flow model. It was shown that the calculation time can be reduced by at least 75 % compared to the detailed model by using the signal flow model. Background is the lower number of state variables to be calculated as well as the significantly reduced parameterization of the signal flow model.

The significantly lower simulation time of the signal flow model becomes especially important when performing variant simulations, for example for parameter optimizations. An external parameter optimization function was used to optimize the linear PID controller. To investigate the potential of the shown modeling approaches for parameter optimizations the function has been applied to both

models. The software concept of the developed optimization function is shown in Figure 11.

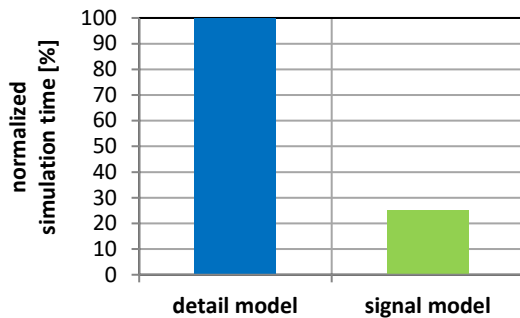


Figure 10: Comparison of simulation time.

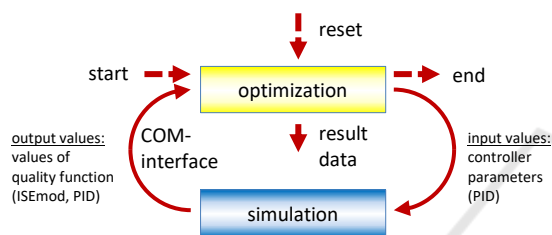


Figure 11: Software concept of the external optimization function, based on (Lohse, 2015).

The simulation program (SimulationX®) is controlled via an existing COM interface by the optimization function of the external program. The function loads the corresponding simulation model and commits the parameters to be optimized - the parameters of the PID controller. After completion of the simulation, the time profiles of the control input (setpoint value) and the control variable (actual value) are transferred to the optimization function. The automated evaluation of the control quality takes place within the optimization function by a modified ISE criterion according to (Lohse, 2015). Thereby  $e$  is the control deviation and  $\dot{e}$  its time derivative.

$$ISE_{mod} = \int_{t_1}^{t_2} e^2 dt + a \cdot \int_{t_1}^{t_2} \dot{e}^2 dt \quad (19)$$

Figure 12 shows the results of the external controller optimization. A robust PID control was designed. A robust control must always be designed at the most unfavorable operating point of the control system. When the main spindle is heavily loaded, the temperature of the spindle shaft and housing increases. It is assumed that a relative thermal expansion of the spindle shaft relative to the housing of maximum  $400 \mu\text{m}$  can take place. Since the oscillation susceptibility of the control loop

increases with increasing thermal expansion, the robust control must be designed for a maximally stretched spindle.

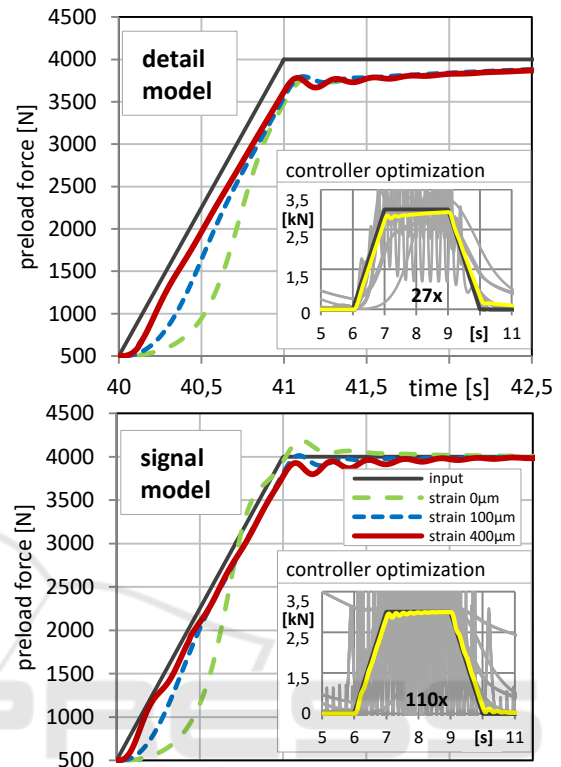


Figure 12: Performance comparison of detail and signal flow model by applying an external parameter optimization function for controller optimization.

For a maximally defined calculation time of both optimization runs, a distinctly coarser interval nesting was used in the application of the detail model, since the calculation time of the detail model for a single simulation run is approximately 4 times higher than that of the signal flow model. The result is a much greater optimization potential of the controller when using the simplified signal flow model. The controller parameterization determined with the signal flow model was tested in the detailed model and led to almost identical simulation results.

## 6 CONCLUSIONS

The presented investigation was part of the research project "Peripherie- und Komponenten-entwicklung für eine adaptronische Hauptspindel" and was carried out at the ICM - Institut Chemnitzer Maschinen- und Anlagenbau e.V. The work deals

with the comparison of different modeling approaches for the simulation of control loop components and control systems in system simulation environments. The aim was to use the example of a valve-controlled hydraulic bearing preload element to investigate how the degree of model detailing affects the controller design of the considered force control and how the simulation performance can be increased by different modeling approaches and model simplifications. Therefore the simulation environment SimulationX® was used.

Controlling element of the investigated control system is a 4/3-way control valve. Different modeling approaches for control valves were examined and compared. It was found that by implementing the experimentally determined 3D flow-maps of the individual control edges into the model, the static transmission behavior of the control valve can be mapped very accurately. Simulation errors less than 5% could be achieved. The second valve model based on the flow-load function and parameterized with the manufacturer's specifications for nominal pressure and nominal volume flow showed only slight deviations from the measured data in a wide range of values. Simulation errors less than 10% could be achieved. Disadvantage of these two models is that they are only applicable to a specific temperature and viscosity of the hydraulic oil. The third control valve model was provided from the model library of SimulationX®. This model shows the lowest accuracy regarding the static transmission behavior compared to the map-based model and the flow-load model. One big advantage of the SimulationX®-model is that the use of empirical equations takes into account the oil viscosity in the description of the flow behavior. The PT2 element on which all three models are based shows a realistic dynamic transmission behavior. This could be shown by comparisons of simulated and experimentally determined frequency and step responses of the control valve.

For the simulative mapping of the overall control system, two modeling approaches have been compared, a detailed physical model and a simplified signal flow model. The detailed physical model shows very realistic simulation results regarding the investigated behavior of the control loop. It was found that by certain reparameterizations of the signal flow model its simulation accuracy can be significantly increased, for example by reparameterization of the control edge overlaps of the control valve model. Overall, a good agreement of the static and dynamic control loop behavior with

the measured data can be achieved with both models. With regard to the needed simulation time the simplified signal flow model is clearly superior to the detail model. The calculation time can be reduced by at least 75 % by using the signal flow model. The higher simulation performance of the signal flow model is particularly evident when using a parameter optimization function to optimize controller parameters. The higher performance of the signal model is even more important if extended control structures are to be designed by means of optimization functions, since a larger number of parameters to be optimized is obtained here. Another disadvantage of the detail model is the significantly greater effort in the model parameterization.

## REFERENCES

- Backhaus, S.-G., 2008. Eine Messstrategie zur Bestimmung des dynamischen Übertragungsverhaltens von Wälzlagern. Göttingen: Cuvillier Verlag Göttingen.
- Harris, T., 2001. Rolling Bearing Analysis. s.l.:John Wiley & Sons.
- Hatami, H., 2013. Hydraulische Formelsammlung. s.l.:Bosch Rexroth Group.
- Ivanov, G., 2018. Detailed modeling of a hydraulic bearing preload element for drive design and control development. Dresden, s.n.
- Lohse, H., 2015. Modellierung hydraulischer Tiefziehpressen für Prozesskopplung, Reglerauslegung und energetische Bilanzierung. Aachen: Shaker Verlag.
- Töpfer, H., Schwarz, A., 1988. Wissensspeicher Fluidtechnik. Leipzig: VEB Fachbuchverlag.
- Weber, J., 2011. Aufbau und Übertragungsverhalten von Stetgiventilen. Studienskript. Dresden: TU Dresden.
- Weber, J., 2011. Übertragungseigenschaften des ventilgesteuerten Zylinderantriebes. Dresden: TU Dresden.